

Multi-Stream Inflation in a Landscape

Francis Duplessis , Yi Wang , Robert Brandenberger
Physics Department, McGill University, Montreal, H3A2T8, Canada

There are hidden observables for inflation, such as features localized in position space, which do not manifest themselves when only one inflation trajectory is considered. To address this issue, we investigate inflation dynamics in a landscape mimicked by a random potential. We calculate the probability for bifurcation of the inflation trajectory in multi-stream inflation. Depending on the shape of the random bumps and the distance between bumps in the potential, there is a phase transition: on one side of the critical curve in parameter space isocurvature fluctuations are exponentially amplified and bifurcation becomes very probable. On the other side bifurcation is dominated by a random walk where bifurcations are less likely to happen.

PACS numbers:

I. INTRODUCTION

During multi-stream inflation [1–4], the classical inflation trajectory bifurcates into multiple branches. Multi-stream inflation provides a possible explanation for features and asymmetries in the CMB, e.g. non-Gaussianities [1, 3], cold spots in the CMB and great voids in the large scale structure [4], and also have a web implication for eternal inflation [2].

Although multi-stream inflation is not necessarily embedded into string theory, the motivation is best understood in terms of the string landscape [5–8]. According to the string landscape paradigm, string theory is unique while the vacuum structure of string theory is extremely complicated. Based on semi-classical investigations of string compactifications one estimates that there are of order 10^{100} or more meta-stable vacua. This forms the string landscape. The implications of the string landscape for inflation should be considered seriously.

Over the past decade there has been a lot of work on inflation in the context of string compactifications (see e.g. [9–11] for some early papers and e.g. [12] for some recent review articles). A lot of the work has focused on specific string theoretical constructions which might yield inflation, and has not taken the landscape features of string theory into account. However, there have been a number of inflation scenarios motivated specifically by the string landscape. An incomplete list includes inflation in a random potential [13–15], chain inflation [16–20], particle production during inflation [21–24], extra symmetry point encounter [25, 26], meandering inflation [27], multi-stream inflation and quasi-single field inflation [28, 29].

In this paper, we focus on multi-stream inflation. It was argued that in the string landscape, where the inflation potential is extremely complicated, bifurcations in the inflation trajectory become possible or even frequent. But no quantitative justifications for this statement were previously provided. The aim of the present paper is to fill this gap, and bring a connection between the landscape and observation.

The observational consequences fall into two possibilities: When the bifurcation probability is rather small, there may be only a few bubbles in the sky following exotic trajectories. In this case multi-stream inflation provides a possible explanation of the cold spot on the CMB, or a void in the large scale structure. On the other hand, when the bifurcation probability is large, extra fluctuations are not under control and thus such random potentials are not consistent with observations – except when they are extremely finely tuned¹, or when the time of bifurcation is pushed to before the observable period of inflation (the final period of inflation during which scales which are currently observed exit the Hubble radius).

The inconsistency for high probability bifurcations in a random potential comes in at least two aspects: Most importantly, different trajectories typically have different e-folding numbers. The e-folding number difference between different trajectories results in an extra fluctuation in the scalar type perturbations. Such a fluctuation with amplitude much greater than 10^{-5} is already ruled out on the scales of CMB. Also, if the different trajectories do not combine or reheat into the same radiation, there will be domain walls in between them, which causes a problem.

In the string landscape the moduli space of low energy modes may have a very large dimension. For simplicity, we assume in this paper that only two fields participate in the dynamics during the inflationary phase. All other flat directions are taken to be stabilized. They do not evolve dynamically but could provide bumps in the effective two

¹ Here we are having in mind a random potential. If the bifurcation potential is not random (say, originate from spontaneous breaking of an approximate symmetry), common bifurcations do not necessarily require a fine tuning.

dimensional landscape. If there were more flat directions taking place in the inflationary dynamics, the bifurcation probability should be larger. Thus, in our present analysis we are actually under-estimating what the bifurcation probability would be in a more general case, perhaps by a huge factor.

The paper is organized as follows: In Section 2, we model the landscape and calculate the bifurcation probability in the landscape analytically. Two cases are considered, either when bifurcations are dominated by an exponential growth of isocurvature fluctuation, or when they are given by a random walk of the isocurvature field. In Section 3, we use stochastic equations to numerically verify the analytical approximations made in the previous section. We discuss our results in Section 4.

II. BIFURCATION PROBABILITIES IN A LANDSCAPE

In this section, we calculate bifurcation probabilities in the landscape. We show that there is a phase transition controlled by the height and the ellipticity of the bumps in the potential.

To model the random potential, we focus on a double-field model. The fields are labeled φ_1 and φ_2 . There is an overall slope in the φ_1 direction, such that if we remove the randomness of the potential, φ_1 becomes the inflation direction and φ_2 has flat potential. To add random features to the potential, we introduce a perturbation U of the potential which is characterized by randomly located and separated bumps. These bumps are characterized by field values $\Delta_p\varphi_1$ and $\Delta_p\varphi_2$ which denote the mean size and separation of the bumps in the φ_1 and φ_2 directions respectively. An ellipticity parameter $\xi \equiv \Delta_p\varphi_1/\Delta_p\varphi_2$ is defined to model the shape of the bumps. The amplitude of the bumps is taken to be the limiting value such that the slow roll condition in the inflaton direction is maintained.

The equations of motion for the fields take the form

$$\ddot{\varphi}_1 + 3H\dot{\varphi}_1 + \partial_1 V(\varphi_1) + \partial_1 U(\varphi_1, \varphi_2) = 0, \quad (1)$$

$$\ddot{\varphi}_2 + 3H\dot{\varphi}_2 + \partial_2 U(\varphi_1, \varphi_2) = 0, \quad (2)$$

where $V(\varphi_1)$ is the slow roll potential, subject to slow roll restrictions, and $U(\varphi_1, \varphi_2)$ is a random potential. Shorthand notations ∂_1 and ∂_2 are used to denote the partial derivatives with respect to the two fields. We use a parameter λ to denote the ratio

$$\lambda \equiv \sqrt{\langle (\partial_1 U)^2 \rangle} / |\partial_1 V|. \quad (3)$$

When $\lambda \ll 1$, the slow roll condition in the inflation direction remains satisfied.

A. Definition of a bifurcation

One subtlety is the question of quantifying what is a bifurcation. We adopt the following two definitions: a bifurcation happens when two sample inflation trajectories (with the same initial conditions):

1. End on different sides of a bump.
2. Are much farther apart at the end of the inflationary phase than would be expected from quantum fluctuations alone.

Numerically, we find that the bifurcation probabilities obtained from these two definitions are practically equal in the interesting region of parameter space. The two definitions give different results when the size of the bumps (both in terms of field extent and height) becomes too small to have any impact on the dynamics. In that case the probability drops to zero for definition 2 while can stay high for definition 1. As we will see, the size when the bumps in the potential become negligible is when they become smaller than the expected quantum fluctuations of the fields. With that insight we define bifurcations based on Definition 2².

² Definitions 1 and 2 also differ when the field extent of the bump is as large as the field distance which the inflaton field moves in of order of a few e-foldings. However, in this case we cannot speak of a random potential any more insofar as the dynamics relevant to cosmological observations is to be considered. Thus, here we are not interested in this situation.

B. Bifurcation from instabilities

Consider two trajectories of φ_2 , denoted by $\varphi_2^{(A)}$ and $\varphi_2^{(B)}$. Let the deviation of these two trajectories as $\delta \equiv \varphi_2^{(A)} - \varphi_2^{(B)}$. Then as long as δ is smaller than $\Delta_p \varphi_2$, one can expand U such that δ satisfies

$$\ddot{\delta} + 3H\dot{\delta} + (\partial_2^2 U)\delta = 0. \quad (4)$$

Now we discuss general features of the potential U . It follows from the classical equation of motion and from the normalization of the density fluctuations produced during inflation that during one e-folding of inflation φ_1 direction rolls a distance of order $10^5 H$.³ This distance is extremely long from the point of view of the field φ_2 , because of the smallness and randomness of the potential U . Thus it is a good approximation to describe the dynamics of φ_2 as taking place in a time-dependent potential given by

$$U(\varphi_1, \varphi_2) = U(\varphi_1(0) + \dot{\varphi}_1 t, \varphi_2), \quad (5)$$

where $\varphi_1(0)$ is the initial value of the field and $\dot{\varphi}_1$ can be treated as a constant.

Over a time interval of a few Hubble times, the field trajectory can pass through a lot of bumps. The number of bumps the field trajectory crosses during a time interval t is about $\dot{\varphi}_1 t / \Delta_p \varphi_1$. Thus, on time scales of order $\Delta_p \varphi_1 / \dot{\varphi}$, the ∂_2^2 parameter in equation (4) will typically change its sign. To model this behavior, we can use the following approximation for the form of the second derivative of the potential $U(\varphi_2, t)$ from (5):

$$\partial_2^2 U \simeq \frac{\lambda \xi \partial_1 V}{\Delta_p \varphi_2} \sin\left(\frac{2\pi \dot{\varphi}_1 t}{\Delta_p \varphi_1}\right). \quad (6)$$

When the sine function change its sign, the equation (4) changes its behavior from oscillation to exponential growth. Now the question is whether the overall behavior shows exponential growth or not. Qualitatively, we see that when the sine function changes its sign slowly enough, there is enough time for growth to take place. On the other hand, when the sign function change its sign extremely quickly, the equation (4) can be treated adiabatically thus there should be no growth.

To be a bit more precise, if we neglect the Hubble friction term for a moment (we will return to the full treatment at the end of this subsection), the equation (4) becomes

$$\ddot{\delta} + \alpha \sin(\beta t) \delta = 0 \quad (7)$$

and thus has the form of the Mathieu equation, the same equation which describes preheating after inflation (see [30, 31] and [32] for a recent review). It will have exponentially growing solutions when

$$|\alpha|/\beta^2 > 0.45 \quad (8)$$

(as shown in figure 1), and non-growing solution otherwise. Note that (8) is the condition for the time scale of the change of the sign of the frequency to be longer than the intrinsic time scale of oscillation.

Inserting the parameters describing the size of the random potential, the condition (8) to have growing solution in the φ_2 direction becomes

$$\left| \frac{\lambda \xi \partial_1 V}{\Delta_p \varphi_2} \right| > 0.45 \left(\frac{2\pi \dot{\varphi}_1}{\Delta_p \varphi_1} \right)^2. \quad (9)$$

Note that the slow roll condition in the inflaton direction implies $|\partial_1 V| \simeq |3H\dot{\varphi}_1|$. Making use of the result $P_\zeta^{1/2} = H^2/(2\pi\dot{\varphi})$ for the power spectrum of cosmological perturbations ζ to eliminate $\dot{\varphi}_1$, the above inequality becomes

$$\frac{\Delta_p \varphi_1}{H} > \frac{1}{\lambda \xi^2 P_\zeta^{1/2}}. \quad (10)$$

When this inequality is satisfied, the solution turns out to be exponentially growing. In order for the exponential growth rate to be large on compared to the Hubble expansion rate we need

$$\left| \frac{\lambda \xi \partial_1 V}{\Delta_p \varphi_2} \right| > H^2. \quad (11)$$

³ This is because, the rolling distance of φ_1 per Hubble time is $\dot{\varphi}/H \sim (H^2/\dot{\varphi})^{-1} \times H \sim P_\zeta^{-1/2} H$.

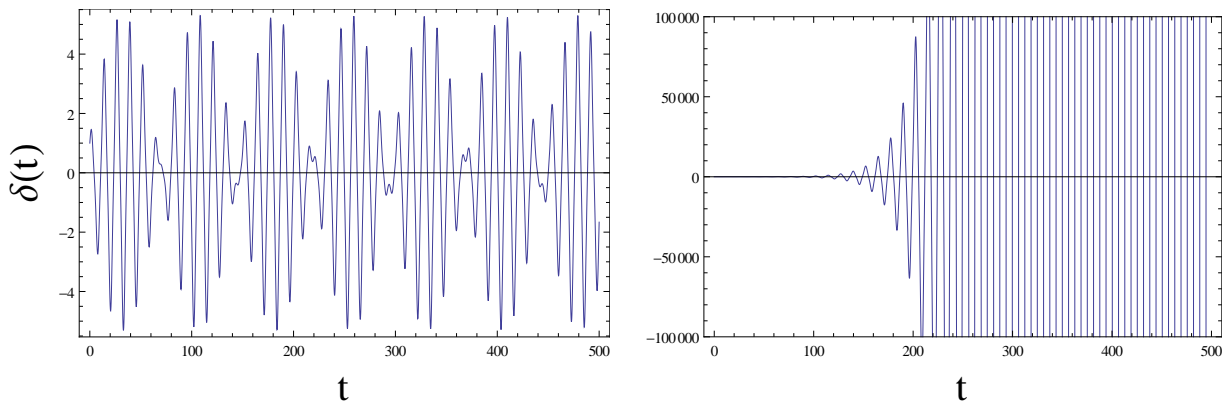


FIG. 1: The behavior of equation $\ddot{\delta} + \alpha \sin(\beta t)\delta = 0$. Here $\beta = 1$ is chosen without loss of generality because varying β is a rescaling of time. The left panel has $\alpha/\beta^2 = 0.45$, and the right panel has $\alpha/\beta^2 = 0.46$. A sharp transition is observed: for $\alpha = 0.45$, the amplitude of δ does not grow, while for $\alpha = 0.46$, the amplitude grows exponentially.

This requirement can be rewritten as

$$\frac{\Delta_p \varphi_1}{H} < \frac{3\lambda\xi^2}{2\pi P_\zeta^{1/2}}. \quad (12)$$

Thus when

$$\frac{1}{\lambda\xi^2 P_\zeta^{1/2}} < \frac{\Delta_p \varphi_1}{H} < \frac{3\lambda\xi^2}{2\pi P_\zeta^{1/2}}, \quad (13)$$

a perturbation in the isocurvature direction will grow until its size reaches the value $\Delta_p \varphi_2$ when bifurcations become common. Note that in terms of ξ , both the inequalities give lower bounds.

Now consider the full equation (4) including the Hubble friction term. Experience from studies of preheating (see [32] for a recent review) teach us that an instability derived in the absence of Hubble friction persists when restoring the friction term: via a field rescaling with a power of the cosmological scale factor the friction term can be eliminated, and the equation of motion of the rescaled variable remains of the type described by Floquet theory and showing an instability.

If there is to be an observable bifurcation, we require that after about 10 e-foldings the growth factor times $H/(2\pi)$ (which is the typical magnitude of quantum fluctuations in a de Sitter phase and which we take to be the initial value of δ) becomes greater than the separation $\Delta_q \varphi_2$ between bumps in the random potential U . This condition can be analyzed numerically, and the result is shown in Figure 2 and Figure 3, as a lower bound on ξ to get bifurcation leading to amplification of the fluctuations. In both figures the area above the curve yields the parameter space for which bifurcations occur and have an observable effect.

From Figure 2, we observe that for small $\Delta_p \varphi_1/H$, one can safely neglect $3H\dot{\varphi}_2$. This is because in that case the oscillations have a much higher frequency than Hubble friction. On the other hand, when $\Delta_p \varphi_1/H$ is large, neglecting $3H\dot{\varphi}_2$ results in an over-estimation of ξ by a factor of 1.7. Figure 3 compares the lower bound for bifurcations obtained using different values of λ .

C. Correction factors

In the previous subsection, we discussed the basic picture of amplified bifurcations in a random potential. However, the model we used is over-simplified, in the sense that there are factors of order one (or order 10) which were ignored. Since we want to relate our analytical analysis to numerical simulations we must discuss the various correction factors

First, as will be discussed in Section III A, the numerical simulations are performed with the maximal amplitude A of the perturbation U of the potential being a function of the bump size, i.e. $A(\Delta_p \varphi_1, \Delta_p \varphi_2)$ (chosen such that the motion in the φ_1 direction is at the borderline of slow rolling). In the analytic calculation this corresponds to working with $\lambda = 1/(10\xi)$.

Second, there is a correction factor along a single inflation trajectory. We have used $\Delta_p \varphi_1$ and $\Delta_p \varphi_2$ to denote the average distance between bumps in the φ_1 and φ_2 directions. However, the criterion for amplified bifurcation is

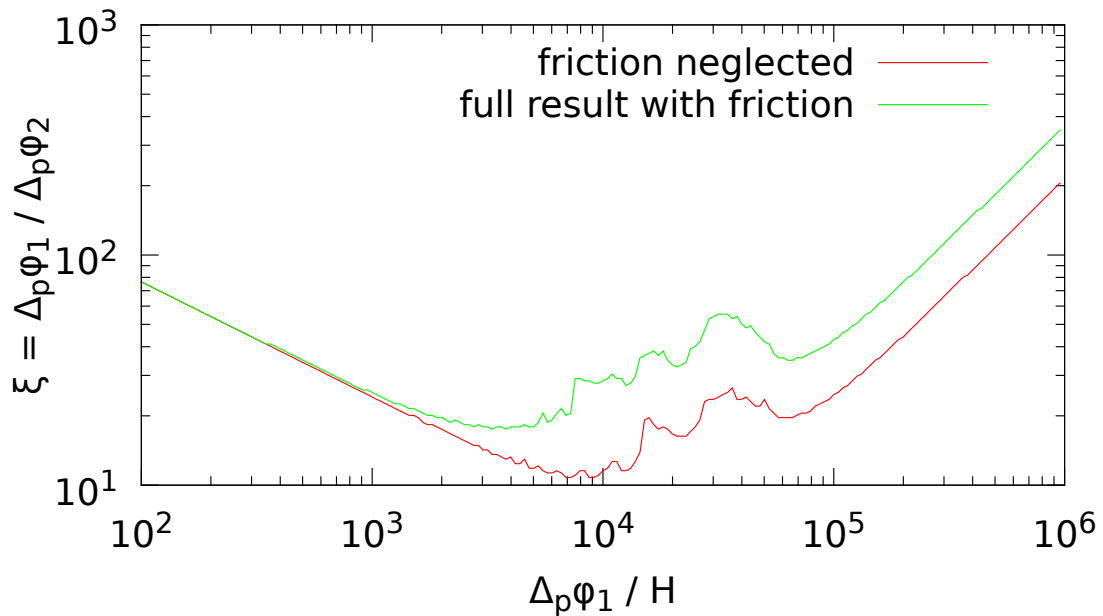


FIG. 2: Comparison between the results neglecting the $3H\dot{\varphi}_2$ term (lower curve) and the full result (upper curve). Here the value $\lambda = 0.1$ is used. The estimate neglecting friction overestimates the bifurcation probability by a factor of up to 1.7 in the variable ξ .

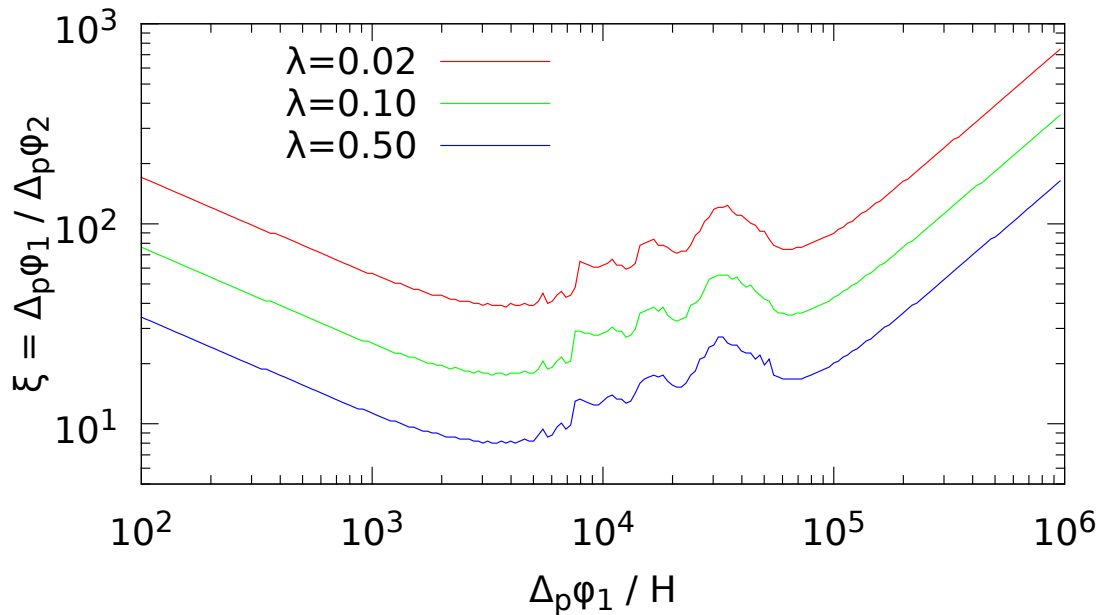


FIG. 3: The lower bound on ξ in order to have bifurcation of the amplification type. Values of ξ above the red, green, blue lines (top line is the red line, bottom line is the blue line) correspond to regions in parameter space where exponential amplification occurs for values of $\lambda = 0.02, 0.10, 0.50$ respectively. In these regions of amplification, the bifurcation probability becomes of order one.

actually not controlled by the average distance, but rather the longest distance between bumps of the same sign in the potential.

To put it more explicitly, along an inflation trajectory, we have assumed that the derivative of the potential in the isocurvature direction $\partial_2 U$ changes its sign when the inflaton rolls an average distance $\Delta_p \varphi_1$. However, a random potential is not exactly periodic. As a result, on a distance of order $n\Delta_p \varphi_1$ (where n is a positive integer), the sign of $\partial_2 U$ as a function of time will be a sequence with length n , like $(+, +, -, +, -, -, -, -, +, \dots)$. The probability of bifurcation is determined by the longest sub-sequence without a sign change (4 in the above example). The

determination of this critical distance is a well defined mathematics problem. Here we do not give an analytical solution. However, numerically, we find that the expectation value (as an ensemble average) of the longest subsequence without sign change $\langle n_{\text{sub}} \rangle$ can be approximated by

$$\langle n_{\text{sub}} \rangle = 1.5 \log(n) , \quad (n \gg 1) . \quad (14)$$

If we are interested in ΔN e-foldings of inflation, n can be written as

$$n = \frac{\dot{\varphi} \Delta N}{H \Delta_p \varphi_1} = \frac{\Delta N}{2\pi \sqrt{P_\zeta}} \frac{H}{\Delta_p \varphi_1} . \quad (15)$$

For example, if we take $\Delta N = 10$, use the CMB normalization of the curvature power spectrum, and take $\Delta_p \varphi_1/H = 100$, we have $n = 324$ and thus $\langle n_{\text{sub}} \rangle = 8.7$. For $\Delta_p \varphi_1/H = 10^3$, we have $\langle n_{\text{sub}} \rangle = 5.2$.

This means that if $\Delta_p \varphi_1$ is the mean size of the bumps in a random potential, then we should compare our numerical simulations to analytic results with bump taken to have size $\langle n_{\text{sub}} \rangle \Delta_p \varphi_1$. Alternatively, if $\Delta_p \varphi_1$ is the size of the bumps in the analytic analysis, we must then compare the analytical results to simulations in a random potential with bumps of mean size $1/\langle n_{\text{sub}} \rangle \Delta_p \varphi_1$. This $\langle n_{\text{sub}} \rangle$ factor yields a correction of the parameters $\Delta_p \varphi_1$, ξ of the form:

$$\Delta_p \varphi_1 \quad \rightarrow \quad \tilde{\Delta}_p \varphi_1 \equiv \frac{1}{\langle n_{\text{sub}} \rangle} \Delta_p \varphi_1 \quad (16)$$

$$\xi \equiv \frac{\Delta_p \varphi_1}{\Delta_p \varphi_2} \quad \rightarrow \quad \tilde{\xi} \equiv \frac{1}{\langle n_{\text{sub}} \rangle} \frac{\Delta_p \varphi_1}{\Delta_p \varphi_2} , \quad (17)$$

and should be used in equations (6) \sim (13). The bifurcation probability using these first two correction factors is plotted in Figure 4. For large $\langle n_{\text{sub}} \rangle$, we have used the above approximated formula (14), and for small $\langle n_{\text{sub}} \rangle$, we have used the explicit result.

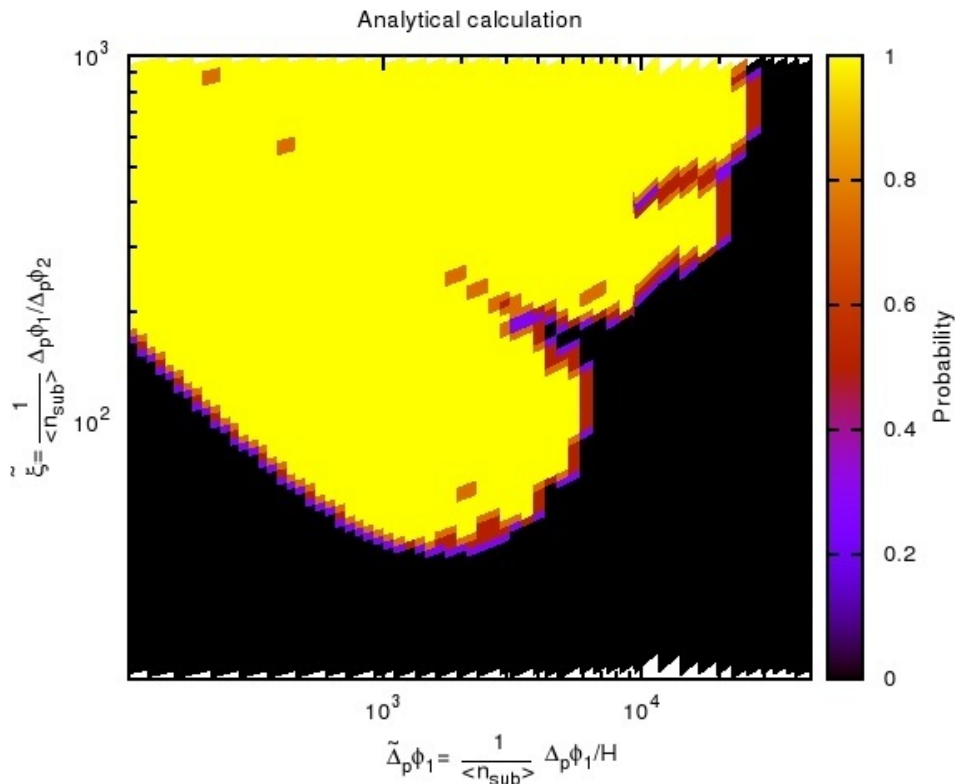


FIG. 4: Probability of bifurcation from analytical calculation simulations. We have rescaled data according to equation (16). Also, a color plot is made for the purpose of comparison with numerical results, with the same set of parameters.

Third, in the previous subsection we were comparing only two trajectories. However, there are exponentially many trajectories (local Hubble volumes) created during inflation. Thus there may be rare bifurcations in some exceptional

trajectories. To take those exceptional trajectories into account, note that the quantum fluctuations are nearly Gaussian and thus given by the following probability distribution

$$\text{Prob} \propto \exp(-\Delta\varphi^2/2\sigma^2) , \quad (18)$$

where σ is the variance of the fluctuations. On the other hand, there are $\exp(3\Delta N)$ trajectories, where ΔN is the e-folding number difference between the bifurcation point and the start of observable inflation. Thus, typically, the largest fluctuation among these $\exp(3\Delta N)$ trajectories is $\Delta\varphi \sim \sigma\sqrt{3\Delta N}$. For example, if we consider $\Delta N = 10$, where bifurcation takes place on the smallest observable scales on CMB, the rare bifurcations could take place even when $\Delta_p\varphi_1$ and $\Delta_p\varphi_2$ are 5 times greater than their critical values.

As mentioned in the introduction, there are big observational differences between the case of rare bifurcations and that of common bifurcations. The case of rare bifurcations could be consistent with current CMB observations and could in fact be responsible for a position space non-Gaussianity. However, if bifurcations become common, fine tuning is needed to make the scenario consistent with observations. This is because in a random potential, different trajectories commonly lead to different number of e-folds of inflation. The difference in e-folding number is translated into temperature anisotropies in the CMB via the δN formalism, which will not be consistent with observations when $\delta N \gg 10^{-5}$.

D. Bifurcation from a Random Walk

Now let us proceed to consider the case in which bifurcations do not lead to an amplification of the isocurvature fluctuations. In this case, we define Δt as the time duration for the field to cross the bump in φ_1 direction. Thus

$$\Delta t = \Delta_p\varphi_1/\dot{\varphi} . \quad (19)$$

During the time interval Δt , the quantum fluctuation in the φ_2 direction is

$$\Delta_q\varphi_2 = \frac{H}{2\pi} \sqrt{H\Delta t} . \quad (20)$$

The bifurcation probability during this Δt time is determined by the ratio

$$\text{Prob}(H\Delta t) = \frac{\Delta_q\varphi_2}{\Delta_p\varphi_2} \quad (21)$$

when $\Delta_q\varphi_2 < \Delta_p\varphi_2$. Otherwise, when $\Delta_q\varphi_2 > \Delta_p\varphi_2$, bifurcations happen frequently, but on the other hand the bumps are too small to lead to interesting consequences.

Now, consider a world line of a comoving observer. The probability for the observer to see bifurcation(s) during N_e e-foldings is

$$\text{Prob}(N_e) = \sum_{n=1}^{N_e/(H\Delta t)} [1 - \sqrt{n}\text{Prob}(H\Delta t)] . \quad (22)$$

The \sqrt{n} factor comes from the random walk accumulation. To have a considerable bifurcation probability, we need

$$\frac{2}{3} \left(\frac{N_e}{H\Delta t} \right)^{3/2} \text{Prob}(H\Delta t) \geq 1 . \quad (23)$$

Inserting numbers, we obtain the following condition for bifurcation

$$\frac{\Delta_p\varphi_1}{H} \leq \sqrt{\frac{N_e^{3/2}\xi}{6\pi^2 P_\zeta^{1/2}}} . \quad (24)$$

For 10 e-foldings, which corresponds to observable scales on the CMB, and for $\xi = 1$, the above inequality is saturated for the value $\Delta_p\varphi_1/H \simeq 100$.

In this subsection, we have not considered the classical dynamics of the φ_2 field. Considering the φ_2 field may encounter a bump and bounce back, we may have over-estimated the bifurcation probability. Moreover, if we impose the slow-roll constraint $\epsilon \ll 1$, bumps formed of Lagrange polynomials will have a negligible effect on the fields compared to quantum fluctuations when $\Delta_q\varphi_2/\Delta_p\varphi_2 \sim 1$. Hence we do not expect any bifurcations if we stick with the definition 2. The conclusion of the current subsection is that, without amplification, bifurcation is less probable to happen in a way which has observational consequences.

III. SIMULATION FOR STOCHASTIC INFLATION

Numerical simulations were performed to obtain the probability of bifurcation in random potentials. The dynamics of our fields are created using Starobinsky's stochastic approach [33] to take into account the quantum fluctuations. In this approach, the equations of motions for φ_1 and φ_2 take the form,

$$\ddot{\varphi}_1(t) + 3H\dot{\varphi}_1(t) + V_{,\varphi_1} = \frac{3}{2\pi}H^{5/2}\eta_1(t), \quad (25)$$

$$\ddot{\varphi}_2(t) + 3H\dot{\varphi}_2(t) + V_{,\varphi_2} = \frac{3}{2\pi}H^{5/2}\eta_2(t). \quad (26)$$

Here the η_i terms are stochastic sources which obey independent Gaussian distributions and are normalized to give

$$\langle \eta_i(t)\eta_i(t') \rangle = \delta(t - t'). \quad (27)$$

To evolve the fields numerically we discretize time in intervals $\Delta t = t_n - t_{n-1}$ so that the delta function becomes

$$\delta(t - t') \rightarrow \frac{\delta_{nm}}{\Delta t}. \quad (28)$$

We do not use the approximations $|\dot{\varphi}_1| \ll |3H\dot{\varphi}_1|$ during the simulation but we did make use of the approximation that the energy density is dominated by the potential in order to write $H = \sqrt{V/3}$.

A. Random Potential

Our random potentials can be written as,

$$V(\varphi_1) + U(\varphi_1, \varphi_2), \quad (29)$$

where V is a background potential that has a small tilt in the φ_1 direction. We chose $V = \frac{1}{2}m^2\varphi_1^2$ for the numerical work. The second term U is a set of random perturbations which are created by discretizing field space (φ_1, φ_2) into a lattice with separation⁴ $\Delta_p\varphi_1$ and $\Delta_p\varphi_2$ and assigning a random number from the interval $[-A, A]$ at each point, and then performing a two dimensional interpolation to obtain a continuous function.

The value of $A(\Delta_p\varphi_1, \Delta_p\varphi_2) > 0$ represents the amplitude of the perturbations and depends on the lattice spacing because we require that the full potential $V+U$ does not lead to violation of the slow-roll condition on the ϵ parameter. This constraint can be made explicit when the form of the perturbations are known. In our case the perturbations are interpolations between the random values associated to each lattice point using a second order Lagrange polynomials.

B. Results

The probability of bifurcation is expressed as a two dimensional plot. The ellipticity ξ and $\Delta\varphi_1/H$ are used to quantify our parameter space.

To achieve a better understanding, two types of potentials are considered: a toy potential with regularly arranged bumps (the left panel of figure 5), and a completely random potential (the right panel of figure 5). The toy potential is faced with the same problem as the analytic model if we want to compare it to the random potential: we must take into account the factor $\langle n_{\text{sub}} \rangle$ and rescale the parameter axes accordingly. The latter is what we want eventually. Note that the figures are only for illustrative purpose, and the actual size of the bumps are much smaller. The results are shown in Figure 6. The plots can be compared with Figure 4, which is obtained from the analytic model.

The shape of the maps from our numerical results and based on the analytical analysis agree with each other when $\Delta_p\varphi_1/H < 10^4$. When $\Delta_p\varphi_1/H > 10^4$, then in the numerical simulations the bifurcation probability decreases, whereas the analytical calculation does not have lead to such a decrease. The difference arises because in the analytical

⁴ A given lattice spacing will represent a potential which is dominated by perturbations whose mean size is of the lattice spacing, hence the use of $\Delta_p\varphi_i$ as notation.

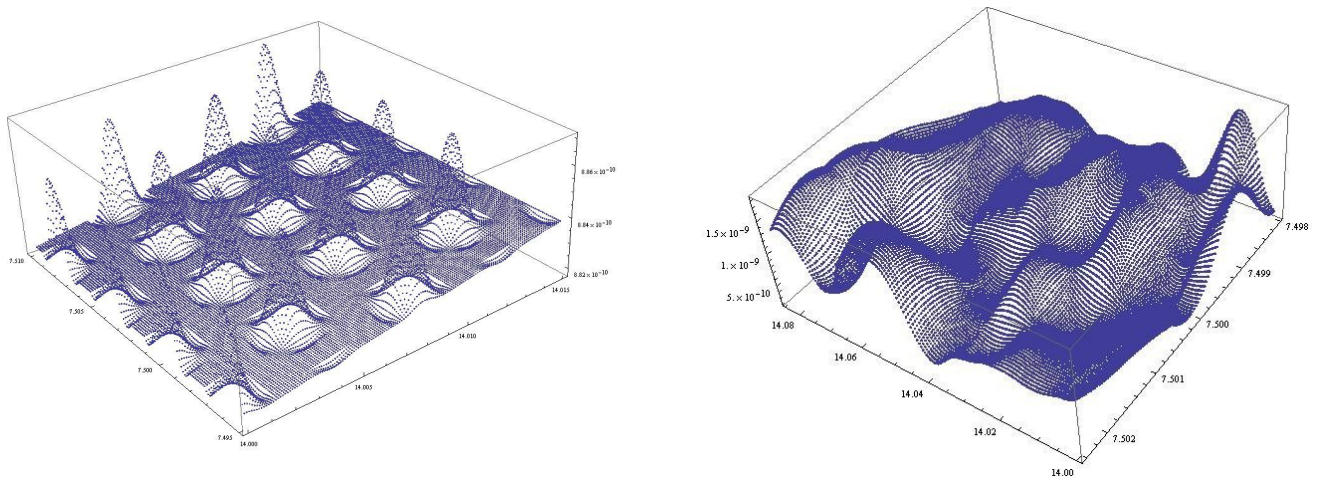


FIG. 5: An illustration of potentials with regularly placed bumps (left panel) and random bumps (right panel). The size of bumps in the actual calculations are much smaller.

analysis we are assuming that the trajectory encounters a large number of bumps. However, when $\Delta_p \varphi_1 / H > 10^4$, the above assumption becomes invalid. We also note that the analytical result under-estimates the bifurcation probability by a factor of about 10.

Using the numerical code, we can also study explicitly what observational problems occur in the case that the bifurcation probability is large. In Figure 7, we show two runs without (left panel) and with (right panel) bifurcations. It is shown that when the bifurcation rate is large, the distribution of e-folding numbers in local patches of the universe becomes highly non-Gaussian, which is not consistent with current observations.

IV. CONCLUSION AND DISCUSSION

To conclude, we have considered the probability of bifurcation of the inflaton trajectory in a (possibly stringy) inflationary landscape. A phase transition from bifurcating dynamics to absence of bifurcations is identified. The phase transition line has been found as a function of the mean distance of the bumps ($\Delta_p \varphi_1 / H$) and of the ellipticity parameter $\Delta_p \varphi_1 / \Delta_p \varphi_2$.

There are a number of interesting questions in this direction which we have not addressed in the present work. For example, the analytical analysis has under-estimated the bifurcation probability by a factor of about 10. Perhaps we are simply using too strong a criterium for bifurcation. But it is also possible that there are other effects leading to bifurcation, that we do not understand currently. Also, in the analysis leading to the results of Figure 4 we only considered the effect from exponential growth of isocurvature perturbations. The random walk may also contribute in the region $\Delta_p \varphi_1 / H < 10^3$. A combined analysis is needed to get a more precise analytical prediction.

As another example, as we mentioned in the introduction, a string landscape could have a large number of modular fields - maybe $\mathcal{O}(100)$. A lot of them may be light and have dynamics. We only considered two of them. It remains interesting to study the behavior in a many-dimensional random potential, and to determine how the bifurcation probability scales as a function of dimension of field space.

Also, a many-dimensional field space opens up the possibility of bifurcation in isocurvature directions. The bifurcation in isocurvature directions could have completely different predictions compared with bifurcations in the curvature direction, and this issue has not been investigated.

In the present work, we have used the separate universe approximation and neglected the field gradient terms. It would be interesting to add those terms back and do a full simulation in position space. Our current analysis does not consider the effect from the boundary regions between bubbles following different trajectories. These regions should become domain walls for a period of time. In the case of rare bifurcations, the trajectories could recombine, and thus there is no domain wall problem. However, it remains interesting to see whether these wall-like objects could lead to observationally interesting predictions, or rule out the whole model.

Finally, in the case of rare bifurcations, i.e. in the parameter regime on the boundary of the black regime in Figures 4 and 6, it would be interesting to see what kinds of bifurcations are more natural in a landscape. The investigation of this question may lead to a more precise correspondence between the string landscape and observations such as the

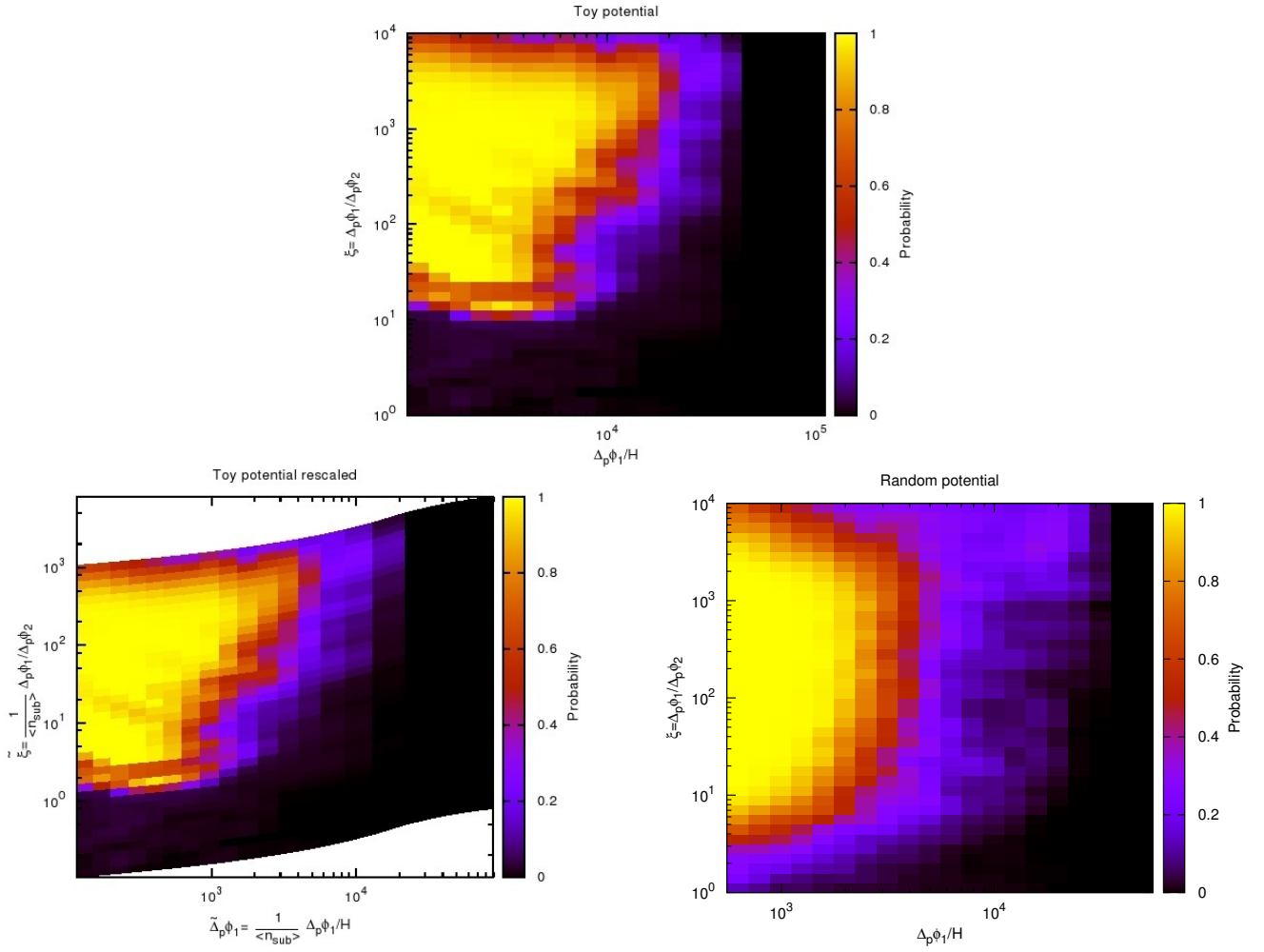


FIG. 6: Probability of bifurcation from numerical simulations. The upper figure is the original result of the toy potential with regularly spaced bumps and the bottom left panel is the same result taking into account the correction factor from $\langle n_{\text{sub}} \rangle$. The bottom right panel is the result for a random potential.

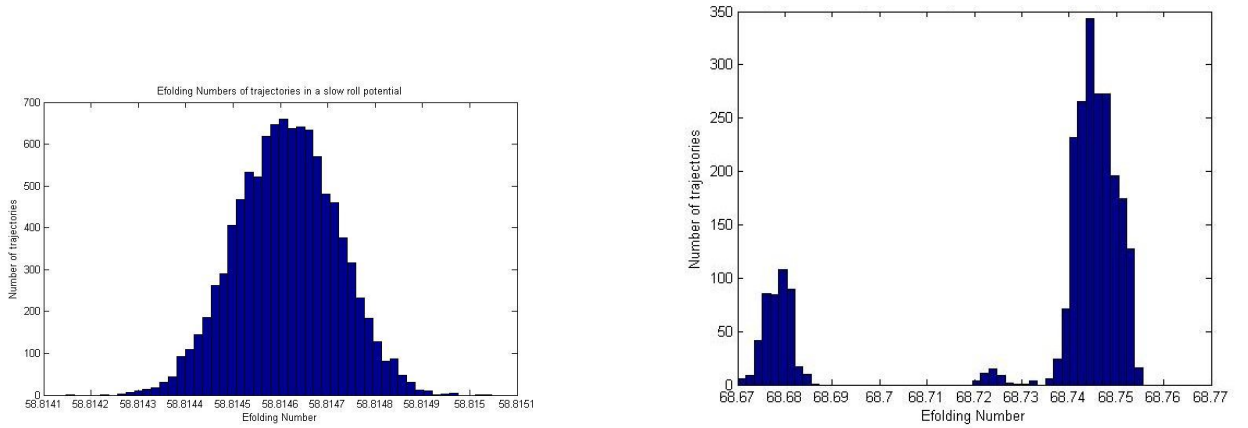


FIG. 7: Probability distribution for the fluctuations based on the δN formalism. The left panel is for trajectories without bifurcation, and the right panel is for trajectories with a large probability of bifurcation, without symmetry protection or fine tuning.

CMB cold spot.

Acknowledgment

This research is supported in part by an NSERC Discovery Grant, by funds from the CRC program, and by a Killam Research Fellowship to RB. YW acknowledges grants from McGill University, the Institute of Particle Physics (Canada) and the Foundational Questions Institute.

-
- [1] M. Li, Y. Wang, “Multi-Stream Inflation,” *JCAP* **0907**, 033 (2009). [arXiv:0903.2123 [hep-th]].
- [2] S. Li, Y. Liu, Y. -S. Piao, “Inflation in Web,” *Phys. Rev.* **D80**, 123535 (2009). [arXiv:0906.3608 [hep-th]].
- [3] Y. Wang, “Multi-Stream Inflation: Bifurcations and Recombinations in the Multiverse,” *Journal of Cosmology*, 2010, Vol 4, pages 744-759 [arXiv:1001.0008 [hep-th]].
- [4] N. Afshordi, A. Slosar, Y. Wang, “A Theory of a Spot,” [arXiv:1006.5021 [astro-ph.CO]].
- [5] R. Bousso and J. Polchinski, “Quantization of four-form fluxes and dynamical neutralization of the cosmological constant,” *JHEP* **0006**, 006 (2000) [arXiv:hep-th/0004134].
- [6] S. B. Giddings, S. Kachru and J. Polchinski, “Hierarchies from fluxes in string compactifications,” *Phys. Rev. D* **66**, 106006 (2002) [arXiv:hep-th/0105097].
- [7] S. Kachru, R. Kallosh, A. Linde and S. P. Trivedi, “De Sitter vacua in string theory,” *Phys. Rev. D* **68**, 046005 (2003) [arXiv:hep-th/0301240].
- [8] M. R. Douglas, “The statistics of string/M theory vacua,” *JHEP* **0305**, 046 (2003) [arXiv:hep-th/0303194].
- [9] G. R. Dvali and S. H. H. Tye, “Brane inflation,” *Phys. Lett. B* **450**, 72 (1999) [hep-ph/9812483].
- [10] S. H. S. Alexander, “Inflation from D - anti-D-brane annihilation,” *Phys. Rev. D* **65**, 023507 (2002) [hep-th/0105032].
- [11] C. P. Burgess, M. Majumdar, D. Nolte, F. Quevedo, G. Rajesh and R. -J. Zhang, “The Inflationary brane anti-brane universe,” *JHEP* **0107**, 047 (2001) [hep-th/0105204].
- [12] C. P. Burgess and L. McAllister, “Challenges for String Cosmology,” *Class. Quant. Grav.* **28**, 204002 (2011) [arXiv:1108.2660 [hep-th]];
L. McAllister and E. Silverstein, “String Cosmology: A Review,” *Gen. Rel. Grav.* **40**, 565 (2008) [arXiv:0710.2951 [hep-th]];
S. H. Henry Tye, “Brane inflation: String theory viewed from the cosmos,” *Lect. Notes Phys.* **737**, 949 (2008) [arXiv:hep-th/0610221];
J. M. Cline, “Inflation from string theory,” hep-th/0501179;
C. P. Burgess, “Inflationary string theory?,” *Pramana* **63**, 1269 (2004) [hep-th/0408037].
- [13] S. -H. H. Tye, J. Xu and Y. Zhang, “Multi-field Inflation with a Random Potential,” *JCAP* **0904**, 018 (2009) [arXiv:0812.1944 [hep-th]].
- [14] N. Agarwal, R. Bean, L. McAllister and G. Xu, “Universality in D-brane Inflation,” *JCAP* **1109**, 002 (2011) [arXiv:1103.2775 [astro-ph.CO]].
- [15] J. Frazer and A. R. Liddle, “Multi-field inflation with random potentials: field dimension, feature scale and non-Gaussianity,” [arXiv:1111.6646 [astro-ph.CO]].
- [16] K. Freese and D. Spolyar, “Chain inflation: ‘Bubble bubble toil and trouble’,” *JCAP* **0507**, 007 (2005) [arXiv:hep-ph/0412145].
- [17] Q. -G. Huang, “Simplified chain inflation,” *JCAP* **0705**, 009 (2007). [arXiv:0704.2835 [hep-th]].
- [18] D. Chialva, U. H. Danielsson, “Chain inflation revisited,” *JCAP* **0810**, 012 (2008). [arXiv:0804.2846 [hep-th]].
- [19] A. Ashoorioon, K. Freese and J. T. Liu, “Slow nucleation rates in Chain Inflation with QCD Axions or Monodromy,” *Phys. Rev. D* **79**, 067302 (2009) [arXiv:0810.0228 [hep-ph]].
- [20] J. M. Cline, G. D. Moore, Y. Wang, “Chain Inflation Reconsidered,” [arXiv:1106.2188 [hep-th]].
- [21] D. J. H. Chung, E. W. Kolb, A. Riotto, I. I. Tkachev, “Probing Planckian physics: Resonant production of particles during inflation and features in the primordial power spectrum,” *Phys. Rev.* **D62**, 043508 (2000). [hep-ph/9910437].
- [22] A. E. Romano, M. Sasaki, “Effects of particle production during inflation,” *Phys. Rev.* **D78**, 103522 (2008). [arXiv:0809.5142 [gr-qc]].
- [23] N. Barnaby and Z. Huang, “Particle Production During Inflation: Observational Constraints and Signatures,” *Phys. Rev. D* **80**, 126018 (2009) [arXiv:0909.0751 [astro-ph.CO]].
- [24] N. Barnaby, “On Features and Nongaussianity from Inflationary Particle Production,” *Phys. Rev. D* **82**, 106009 (2010) [arXiv:1006.4615 [astro-ph.CO]].
- [25] D. Battfeld, T. Battfeld, “A Terminal Velocity on the Landscape: Particle Production near Extra Species Loci in Higher Dimensions,” *JHEP* **1007**, 063 (2010). [arXiv:1004.3551 [hep-th]].
- [26] D. Battfeld, T. Battfeld, C. Byrnes, D. Langlois, “Beauty is Distractive: Particle production during multifield inflation,” *JCAP* **1108**, 025 (2011). [arXiv:1106.1891 [astro-ph.CO]].
- [27] S. -H. H. Tye, J. Xu, “A Meandering Inflaton,” *Phys. Lett.* **B683**, 326-330 (2010). [arXiv:0910.0849 [hep-th]].
- [28] X. Chen, Y. Wang, “Large non-Gaussianities with Intermediate Shapes from Quasi-Single Field Inflation,” *Phys. Rev.* **D81**, 063511 (2010). [arXiv:0909.0496 [astro-ph.CO]].

- [29] X. Chen, Y. Wang, “Quasi-Single Field Inflation and Non-Gaussianities,” JCAP **1004**, 027 (2010). [arXiv:0911.3380 [hep-th]].
- [30] J. H. Traschen and R. H. Brandenberger, “Particle Production During Out-of-equilibrium Phase Transitions,” Phys. Rev. D **42**, 2491 (1990);
Y. Shtanov, J. H. Traschen and R. H. Brandenberger, “Universe reheating after inflation,” Phys. Rev. D **51**, 5438 (1995) [hep-ph/9407247].
- [31] L. Kofman, A. D. Linde and A. A. Starobinsky, “Towards the theory of reheating after inflation,” Phys. Rev. D **56**, 3258 (1997) [hep-ph/9704452].
- [32] R. Allahverdi, R. Brandenberger, F. -Y. Cyr-Racine and A. Mazumdar, “Reheating in Inflationary Cosmology: Theory and Applications,” Ann. Rev. Nucl. Part. Sci. **60**, 27 (2010) [arXiv:1001.2600 [hep-th]].
- [33] A. A. Starobinsky, “Stochastic De Sitter (inflationary) Stage In The Early Universe,” In *De Vega, H.j. (Ed.), Sanchez, N. (Ed.): Field Theory, Quantum Gravity and Strings*, 107-126.